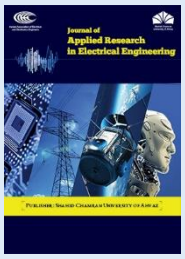
Shahid Chamran University of Ahvaz

Iranian Association of Electrical and Electronics Engineers

Journal of Applied Research in Electrical Engineering

E-ISSN: 2783-2864
P-ISSN: 2717-414X
Homepage: https://jaree.scu.ac.ir/



Research Article/ Review Article/ Applied Article

Coordinated Application of Flux-Coupling SFCLs and Passive Mechanical DC Circuit Breakers for Enhanced HVDC Fault Protection

Ali Kamali[1], S. Masoud Barakati[1,*]

[1] *Faculty of Electrical and Computer Engineering, University of Sistan and Baluchestan, Zahedan, Iran*

* *Corresponding Author: S. Masoud Barakati(smbaraka@gmail.com)*

Abstract: Interrupting current in high-voltage direct current (HVDC) networks is one of the most challenging protection issues in modern DC systems, due to the absence of a natural zero-crossing and the extremely rapid rise of fault current (*di/dt*). Limiting the fault current magnitude, providing an appropriate commutation path, and safely absorbing fault energy are among the most demanding requirements in the design of DC circuit breakers (DCCBs). One effective approach to mitigate these stresses is the synergistic integration of flux-coupling superconducting fault current limiters (FC-SFCLs) with passive mechanical circuit breakers (P-MCBs). This paper investigates a modified flux-coupling-type SFCL (FC-SFCL) and evaluates its effectiveness in the successful operation of passive mechanical circuit breakers (P-MCBs) in HVDC systems. The approach combines the advantages of resistive SFCLs (fault current magnitude reduction) and inductive SFCLs (slowing the *di/dt*) simultaneously. First, the operating principles of the FC-SFCL and P-MCB are examined, and then the impact of the FC-SFCL is analyzed through simulations under two fault scenarios: close and distant from the P-MCB. Simulation results show that an appropriately designed FC-SFCL can reduce the peak fault current by about 37% under far-end faults and up to 80% under near-end faults, resulting in a significant reduction in the required commutation capacitance and enhanced interruption performance. The integration of this SFCL with P-MCBs can provide a promising pathway for developing fast, low-stress, and reliable protection solutions in future HVDC networks.

Keywords: HVDC systems, DC circuit breaker (DCCB), Superconducting fault current limiter (SFCL), Flux-coupling SFCL (FC-SFCL), Passive mechanical circuit breaker (P-MCB).

Article history
Received 24 May 2026; Revised 20 June 2026; Accepted 05 July 2026; Published online 20 September 2026.
© 2026 Published by Shahid Chamran University of Ahvaz & Iranian Association of Electrical and Electronics Engineers (IAEEE)
How to cite this article
A. Kamali, and S. Masoud Barakati, " Coordinated Application of Flux-Coupling SFCLs and Passive Mechanical DC Circuit Breakers for Enhanced HVDC Fault Protection," *J. Appl. Res. Electr. Eng.*, vol. 4, no. 2, pp. 254-265, 2025.
DOI: https://doi.org/10.22055/jaree.2026.52186.1314

Check for updates

Abbreviation	Definition
HVDC	High Voltage Direct Current
MVDC	Medium Voltage Direct Current
DCCB	DC Circuit Breaker
P-MCB	Passive Mechanical Circuit Breaker
FC-SFCL	Flux-Coupling Superconducting Fault Current Limiter
R-SFCL	Resistive Superconducting Fault Current Limiter
MOV	Metal Oxide Varistor
IGBT	Insulated Gate Bipolar Transistor
IGCT	Integrated Gate-Commutated Thyristor
L_1, L_2	Self-inductances of the coupled coils
M	Mutual inductance between the coupled coils
M	Main Circuit Breaker
k	Magnetic coupling coefficient

I_{Line}	Line current
I_M	Main breaker branch current
I_{ax}	Auxiliary branch current
C_{ax}	Auxiliary commutation capacitance
di/dt	Rate of rise of fault current
P_0	Arc power loss parameter in the Mayr model
τ	Arc time constant
g	Arc conductance
V_{arc}	Arc voltage
Z_{CT}	Equivalent impedance of the FC-SFCL
I^2t	Specific energy associated with fault current interruption

1. INTRODUCTION

In DC faults, the extremely rapid rise of fault current subjects DC circuit breakers (DCCBs) to high current peaks and significant energy dissipation during the interruption process. A key concept to mitigate these stresses is the use of superconducting fault current limiters (SFCLs), which reduce both the fault current and its rate of rise (di/dt) before the DCCB initiates interruption [1]. In other words, the SFCL acts as a "fault conditioner," enabling the breaker to operate under lower stress and with a safer margin. Therefore, selecting an appropriate SFCL capable of providing the required conditions for interruption within a very short time is critical.

Early studies on flux-coupling SFCLs (FC-SFCLs) mainly focused on AC power systems, aiming to improve transient stability and reduce network instability risks [2]. These configurations typically employed a hybrid flux-coupling SFCL with a resistive superconducting element that quenched during faults, thereby increasing the device impedance. This approach demonstrated the potential of SFCLs in reducing instability risks.

With the development of DC systems, the need for rapid fault current limitation with di/dt rates reaching tens of kA/ms emerged. In this context, hybrid flux-coupling SFCLs with resistive YBCO elements have gained attention. Reference [3] presents a conceptual electromagnetic design and simulation of an FC-SFCL applied for protection against multiple short-circuit fault scenarios in ships. The results show effective fault current limitation on both AC and DC sides, reducing DC peak currents from approximately 87 kA to 10 kA. The current limiting ratios were about 95% for AC faults and 87.5% for DC faults, confirming the practical feasibility of FC-SFCLs in MVDC systems.

Reference [4] provides a fundamental comparison between conventional inductive FC-SFCLs and resistive types in HVDC systems, indicating that resistive SFCLs are more advantageous from the HVDC perspective. In [5], a modified flux-coupling design is proposed to mitigate DC short-circuit faults in VSC-HVDC systems. A 100 kV VSC-HVDC system equipped with SFCL was simulated in MATLAB/Simulink, demonstrating that the addition of the SFCL reduces DC fault currents and improves DC voltage sag during faults.

References [6] and [7] further explore FC-SFCLs with two parallel windings. The studies show that parallel winding configurations influence operational indices such as fault current, limiting impedance, and instantaneous power. Moreover, the use of a dual-quench mechanism improves temporary fault current limitation and post-fault recovery, making current suppression more effective. In reference [8], a flux-coupled SFCL-CB was proposed to effectively limit DC fault currents and reduce the stress on the circuit breaker. The proposed di/dt-based protection algorithm also improves coordination with protective relays and prevents unnecessary operation during load fluctuations. Reference [9], a modified flux-coupling-type superconducting fault current limiter (MFC-SFCL) was developed to improve fault current limiting performance in VSC-HVDC networks. The proposed design was validated through coupled electromagnetic–thermal finite element simulations, providing a comprehensive evaluation of its current-limiting capability and multiphysics behavior under fault conditions. References [10] The FC-SFCL primarily improves the fault ride-through (FRT) capability of renewable energy sources by limiting AC-side fault currents, whereas the optimized Voltage-Dependent Current Order Limiter (VDCOL) mitigates commutation failures and prevents HVDC blocking. The coordinated operation of these technologies effectively suppresses cascading fault propagation while maintaining power balance in AC/DC hybrid power systems.

Overall, while flux-coupling or flux-lock-based SFCLs show promise in power systems, structural modifications—particularly the addition of resistive elements—can significantly enhance performance in MVDC and HVDC networks. This study not only compares the modified FC-SFCL with the baseline model but also evaluates its integration with passive resonant DC circuit breakers (P-MCBs) to address one of the critical challenges of MVDC/HVDC networks: ultra-fast DC fault current mitigation. The results demonstrate that the FC-SFCL, by "conditioning the fault" and simultaneously reducing current peaks and di/dt, can substantially lower transient stresses and energy dissipation in the interruption path, effectively improving the DCCB's reliability and interrupting capability under both near and distant fault conditions. A comparison of the present study with previous works is summarized in Table 1. As shown in Table 1, most existing studies have focused on the standalone analysis of SFCLs or on evaluating their current-limiting capabilities, while realistic modeling of DC circuit breakers, particularly considering arc dynamics, has rarely been addressed. In this study, a multi-level validation framework is presented, which includes: the fundamental operating principles of the FC-SFCL, detailed physical modeling in COMSOL, and system-level implementation in PSCAD. This approach enables a realistic qualitative assessment of FC-SFCL performance in DC systems. Key Contributions and Novelty:

- **Development of an arc-based model for passive mechanical DC circuit breakers (P-MCBs), enabling realistic simulation of the interruption process and arc extinction dynamics.**
- **Investigation of the role of superconducting fault current limiters (SFCLs) in enhancing HVDC system protection and improving breaker interruption performance.**
- **Quantitative evaluation of FC-SFCL fault-current conditioning capability, showing fault current reductions of up to 80% for near-end faults and 37% for remote faults, together with a significant decrease in the current rise rate (di/dt) and interruption stresses imposed on the P-MCB.**
- **Comparative analysis of HVDC system performance with and without SFCL integration under different fault conditions.**
- **Integration and coordinated operation of a flux-coupling superconducting fault current limiter (FC-SFCL) with a passive mechanical DC circuit breaker (P-MCB) for improved fault interruption capability.**

- **Development of a multi-level COMSOL–PSCAD simulation framework for electromagnetic modeling of the FC-SFCL and transient analysis of HVDC fault scenarios.**

Table. 1. Comparison of the present study with previous works.

Ref.	System Type	SFCL Type	DCCB Modelling	Fault Scenario	Analysis Metrics	Study Type	Key Findings	Limitations / Gaps
[3]	MVDC (Shipboard)	FC-SFCL	✗	AC/DC fault	I_{peak}	Simulation	Effective limitation (~87%)	DCCB not considered
[4]	HVDC	R-SFCL vs FC-SFCL	✗	DC fault	Stability	Comparative	R-SFCL superior in HVDC	No breaker analysis
[5]	VSC-HVDC	Modified FC-SFCL	✗	DC fault	I_{fault}, V_{dc}	Simulation	Improved voltage and reduced current	No interaction with CB
[6]	DC	FC-SFCL (parallel SC)	✗	DC fault	Impedance, Power	Experimental	Effect of winding/flux coupling	Lacks protection analysis
[7]	DC	Flux-Lock (Twice Quench)	✗	DC fault	I_{peak}, Limiting time	Experimental	Improved limiting duration	Temporary limitation only
[8]	DC	Flux-Coupled SFCL-CB	Simplified CB	DC fault	Ipeak, di/dt	Simulation	Reduced CB stress and improved protection	limited interruption analysis
[9]	VSC-HVDC	Modified FC-SFCL	✗	DC fault	Ifault , thermal electromagnetic behavior	FEM	Improved limiting, validated through multiphysics modelling	No circuit breaker interaction or interruption study
[10]	AC/DC Hybrid Grid with HVDC	FC-SFCL + Optimized VDCOL	✗	N-1 and N-2 faults	Ifault, FRT, HVDC power transfer	System-level simulation	Reduced fault currents (~50%), prevented cascading faults, improved FRT and HVDC operation	Focused on AC-side stability; no DCCB modelling
Summary	Most existing studies	FC-, Modified FC-, or Flux-Lock SFCL	✗ or highly simplified	Single fault scenario	Primarily fault current reduction	Simulation / Experimental	Focus on SFCL design and current-limiting capability	Realistic DCCB behaviour, arc dynamics
This Work	HVDC (100 kV)	FC-SFCL + Modified FC-SFCL (Comparison)	Arc-based P-MCB model	Near-end & Far-end DC faults	Ipeak, di/dt, interruption stress, arc dynamics, LC design	Multi-level (COMSOL + PSCAD)	Demonstrates fault conditioning, reduction of fault current (up to 80% near faults and 37% remote faults), reduced stress and improved interruption performance	

Furthermore, the dynamic interaction between the FC-SFCL and the DCCBs is analyzed in detail. The results show that fault conditioning can directly reduce commutation path requirements and breaker energy stress. This methodology not only demonstrates the effectiveness of FC-SFCLs under various fault scenarios but also provides an engineering approach to lower the demands for ultra-fast DC breaker operation and mitigate high *di/dt* challenges in DC systems. Consequently, a more economical and reliable HVDC protection design is achieved, offering significant scientific and industrial value. In this study an equivalent HVDC network models and fixed arc parameters are used to focus on the fundamental interaction between the FC-SFCL and the DC circuit breaker.

2. Operating Principles and Relations

This section presents the operating principles of the main components of the studied protection system, including the flux-coupling superconducting fault current limiter (FC-SFCL) and the passive mechanical circuit breaker (P-MCB). The aim is to provide a physical understanding and fundamental modeling of their behavior under DC fault conditions, as well as to clarify their roles in current limiting and interruption processes. First, the operating mechanism of the FC-SFCL is discussed as a pre-fault current limiting device, which operates based on magnetic coupling and the dynamic behavior of superconductors. Next, the operation of the passive mechanical circuit breaker is analyzed, focusing on its role in extinguishing the arc and achieving current zero. This separation allows a clear distinction between the fault-conditioning role of the FC-SFCL and the final interruption process by the P-MCB, enabling a more detailed analysis of the interaction between these two components in DC networks.

2.1. Flux-Coupling SFCL (FC-SFCL)

Two magnetically coupled inductors can be configured in either additive (aiding) polarity or subtractive (opposing) polarity, depending on the winding direction of the primary and secondary coils on the iron core. This configuration affects the transient behavior. It also changes the effective fault impedance. Consequently, it influences the current-limiting performance. As illustrated in Fig. 1, two coupled

inductors with self-inductances L_1 and L_2 and mutual inductance M are connected in parallel. In the case of additive polarity (Fig.1a), the fluxes generated in the core are in the same direction, reinforcing the coupling. As a result, the equivalent inductance increases, and the impedance seen by the circuit is higher Conversely, in the subtractive polarity case (Fig.1b). The fluxes oppose each other. This leads to partial cancellation. This leads to a lower equivalent inductance and reduced effective impedance. These two arrangements form the basis of flux-lock/flux-coupling behavior in FC-SFCLs. They enable significant impedance variation between normal and fault conditions [11]. As shown in Fig. 2, the equivalent representation of two magnetically coupled inductors with opposing polarity is presented. In this configuration, the coupling effect appears in a subtractive form. The effective inductances of the branches are represented as $L_1 + M$ and $L_2 + M$. A central branch with value $-M$ represents mutual interaction. The negative sign of $-M$ indicates that the induced voltage opposes the self-induced voltage. This results in partial flux cancellation.

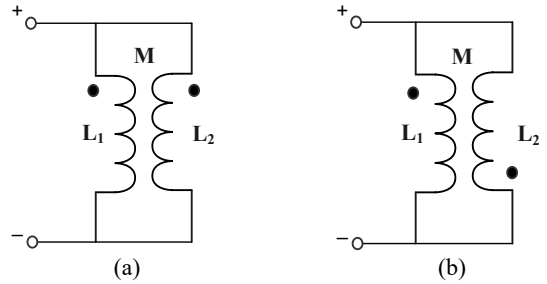


Fig. 1. Parallel-connected mutually coupled inductors with self-inductances L_1 and L_2 and mutual inductance M: (a) additive polarity, (b) subtractive polarity.

As a result, the equivalent inductance is reduced. The circuit impedance also decreases. Consequently, the system responds faster to rapid current changes.

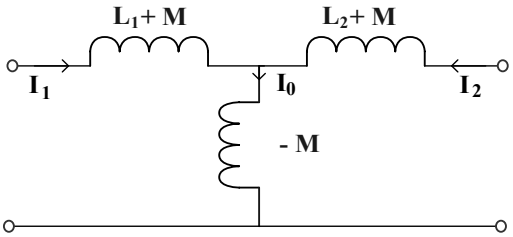


Fig. 2. Equivalent representation of mutually coupled inductors with opposing polarity, where the coupling effect is modeled by branch inductances $L_1 + M$ and $L_2 + M$ and a mutual component $-M$.

This equivalent model forms the basis for the mathematical analysis of the coupling effect. It uses $M = k\sqrt{L_1 L_2}$. It is also used to study FC-SFCL impedance variation across operating states. The ± sign depends on winding direction and polarity.

$$V_1 = L_1 (di_1 / dt) \pm M (di_2 / dt) \quad (1)$$

$$V_2 = L_2 (di_2 / dt) \pm M (di_1 / dt) \quad (2)$$

$$M = k\sqrt{(L_1 L_2)} \quad (3)$$

$$Z_{CT} = \frac{j\omega(L_1 L_2 - M^2)}{(L_1 + L_2 + 2M)} \quad (4)$$

This fundamental behavior forms the basis of the flux-coupling type SFCL as a fault current limiter.When the coupling coefficient is close to unity ($K \approx 1$), the SFCL remains nearly transparent to the system during normal operation. Under fault conditions, it presents a higher impedance that limits the fault current.

Fig. 3 illustrates the equivalent model of a flux-coupling SFCL based on two coupled coils with self-inductances L_1 and L_2 and mutual inductance M**.** Fig. 3(a) shows the basic FC-SFCL topology, including a control switch S_1 for enabling/disabling the flux-lock path and a metal-oxide varistor (MOV) for mitigating transient overvoltages. Fig. 3(b) presents the modified model, which incorporates a series superconducting/limiting element in the main path to enhance the damping component and improve current-limiting performance under DC fault conditions [12], [13]. The flux-coupling type SFCL (FC-SFCL) is designed based on a differential polarity coil coupling mechanism. Under normal operating conditions, the controlled switch is closed, and the coils remain superconducting. The coils are wound in opposing directions on a common iron core. A high coupling coefficient (k ≈ 1) maximizes the magnetic coupling. Under normal operating conditions, the magnetic fluxes largely cancel each other. This minimizes losses and impedances. As a result, the coils exhibit non-inductive coupling behavior.

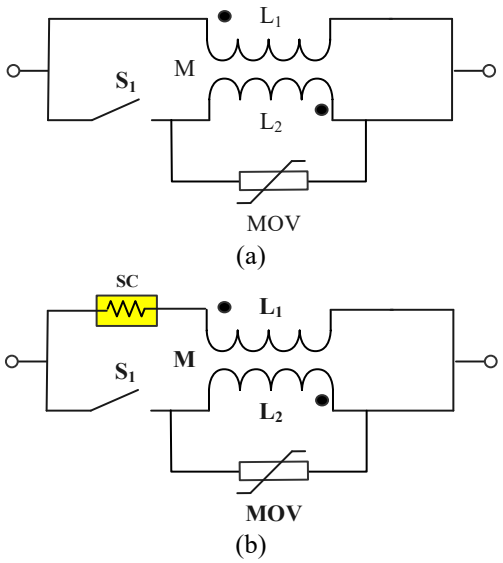


Fig. 3. FC-SFCL equivalent circuits: (a) baseline flux-coupled model with switch S_1 and MOV; (b) modified model with an added superconducting/limiting element for improved DC fault current limitation.

As a result, the effective impedance is very small (near zero), and the device has negligible impact on the main circuit.

$$k \to 1 \Rightarrow Z_{CT} \to 0 \quad (5)$$

$$Z_{SFCL} \approx 0 \quad (6)$$

Upon fault detection, the switch S_1 is opened at a very high speed. High-power semiconductor devices, such as IGBTs or IGCTs, are typically used for this purpose. These devices provide high current and voltage ratings together with fast switching capability. When the switch operates, the non-inductive coupling between the coils is disrupted. As a result, a limiting impedance is introduced into the circuit. This impedance can be approximately expressed as:

$$Z_{SFCL} \approx j\,\omega L_2 \quad (7)$$

This impedance reduces the fault current and helps control the rate of rise (*di/dt*). One of the challenges of non-quenched FC-SFCLs is that they may not sufficiently limit the fault current peak. To address this limitation, a quench-based design is proposed. In this design, a resistive element is added to the inductive path. The added resistance suppresses the fault current peak. It also increases the overall impedance. As a result, the interruption burden on the main circuit breaker is reduced.

$$Z_{SFCL} \approx R_{SC} + j\,\omega L_2 \quad (8)$$

Once the transient period ends, the DC current reaches steady state ($\omega = 0$). Consequently, the circuit impedance becomes purely resistive. This impedance helps maintain the fault current amplitude at a controlled and manageable level [2].

$$Z_{SFCL} \approx R_{SC} \quad (9)$$

2-2) Passive Mechanical Circuit Breaker (P-MCB)

For simulating the operation of a passive mechanical circuit breaker (*P-MCB*), it is necessary to use an arc model instead of an ideal switch model [14]. Electrical arc models are generally based on the dynamic behavior of arc conductance or resistance. Depending on the modeling requirements, different arc models can be employed. The most widely used models are the Cassie, Mayr, and Cassie–Mayr hybrid models.

These models can accurately simulate the dynamic behavior of arcs in DC circuit breakers. The Mayr model is particularly suitable for low-current regions and around the current zero crossing [15]. Its main equation is expressed as:

$$\frac{1}{g}\frac{dg}{dt} = \frac{1}{\tau}\left(\frac{ui}{P_0} - 1\right) \quad (10)$$

where g *is* the arc conductance, u is the arc voltage, i is the arc current, P_0 is the arc constant power loss, and τ is the arc time constant. Since $u = i.g$ the arc conductance varies dynamically. In the Mayr model, if the input power ui exceeds the arc losses P_0, the arc is reinforced, whereas if it is lower than P_0, The arc extinguishes. The Cassie model is more suitable for high-current regions. Its governing equation is expressed as:

$$\frac{1}{g}\frac{dg}{dt} = \frac{1}{\tau}\left(\frac{u^2}{U_C{}^2} - 1\right) \quad (11)$$

Where g is the arc conductance, u is the arc voltage, U_c is the Cassie voltage constant, τ is the arc time constant. This formulation emphasizes the exponential growth or decay of arc conductance depending on whether the instantaneous power exceeds or falls below the reference power level. A key feature of the Cassie model for high currents is that the arc channel temperature is assumed to be nearly constant, and variations in the plasma diameter are taken into account. In the Cassie–Mayr hybrid model, which is widely used in PSCAD simulations and HVDC studies, the Cassie model governs the behavior at high currents, while the Mayr model accurately reproduces the arc dynamics near current zero [16], [17]. The general form of the hybrid model is expressed as:

$$g = \alpha g_{Cassie} + (1-\alpha)\, g_{Mayr} \qquad 0 \le \alpha \le 1 \quad (12)$$

In PSCAD/EMTDC, the Breaker Arc module employs the Cassie–Mayr dynamic arc model. Unlike ideal switch models, it considers the transient behavior of the arc during current interruption. When the breaker contacts separate, an electrical arc is formed. The arc remains until extinction occurs. During this period, the arc conductance changes continuously with the arc conditions. The governing equations are solved in the EMTDC discrete-time framework. Therefore, the arc conductance is updated at each simulation time step, Δt, as follows:

$$g[n+1] = g[n] + \Delta t.\frac{dg}{dt} \quad (13)$$

where $g[n]$is the arc conductance at time step n, and $\Delta t$is the simulation time step. The derivative $\frac{dg}{dt}$ is determined based on the selected arc model (Mayr, Cassie, or Cassie–Mayr hybrid model). Electrical arc models are generally based on the dynamic behavior of arc conductance or resistance. Common examples include the Cassie, Mayr, and Cassie–Mayr hybrid models. At each step, the arc resistance is updated as:

$$R_{arc}(t) = \frac{1}{g(t)} \quad (14)$$

where $g(t)$ is obtained from the dynamic arc equations [18]. In this study, the Mayr model is adopted for the operation of the passive mechanical circuit breaker, since it provides a more accurate representation of arc extinction near current zero, which is a critical operating region for mechanical DC circuit breakers. Fig. 4 illustrates the adopted formulation and the corresponding modeling framework.

Fig. 5 illustrates the modeling structure of the passive mechanical circuit breaker (P-MCB) together with the arc model. As shown in Fig. 5(a), the breaker consists of the main switch M, a parallel auxiliary branch controlled by switch K_1, and a metal-oxide varistor (MOV) used as an energy absorption element. The auxiliary branch provides an alternate current path during interruption. This reduces the current through the main switch and drives it toward zero. Meanwhile, the MOV limits the overvoltage generated during interruption. This protects the switching components and other system equipment. Fig. 5(b) presents the dynamic switch model. In this model, the circuit breaker is not represented as an ideal switch. Instead, the processes of arc formation and extinction are explicitly considered. The main switch *M* is modeled using an arc model block characterized by (τ, P_0). This block reproduces the transient arc behavior during contact separation. The electric arc is represented by a time-varying resistance, R_{arc}. Its value depends on the arc conductance and energy balance. This sub-model enables the analysis of the arc voltage V_{arc}. It also captures the evolution of arc resistance and the current transfer process to the auxiliary branch. As a result, the proposed model accurately reproduces the current extinction process. It also reflects the realistic behavior of the mechanical circuit breaker during DC interruption [16].

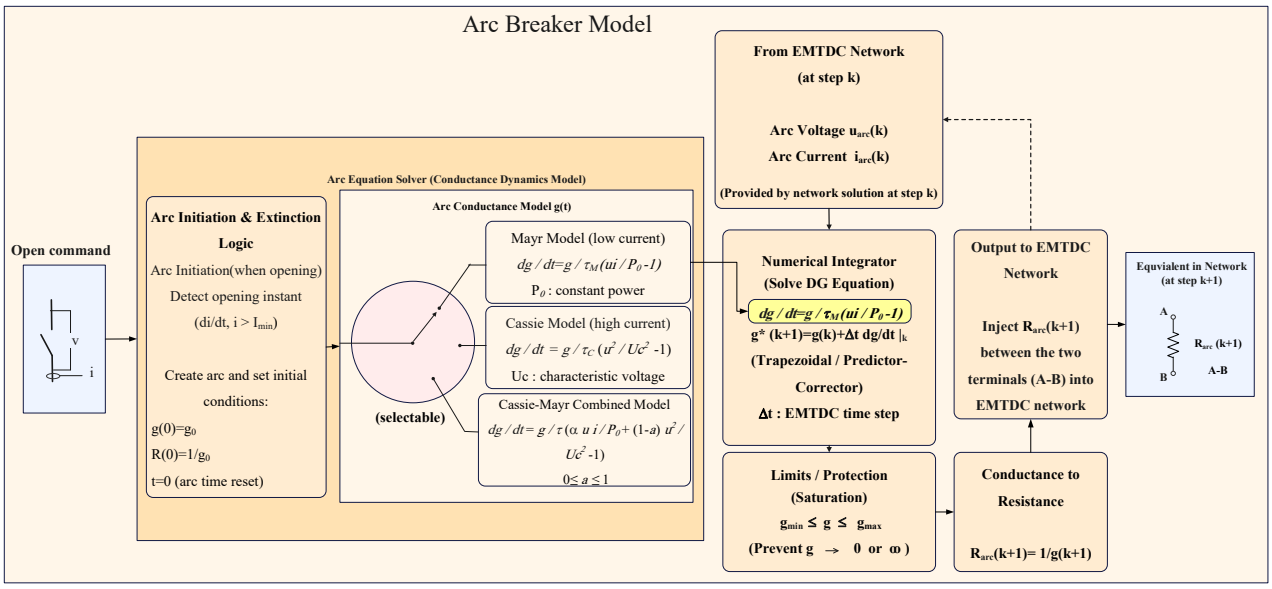
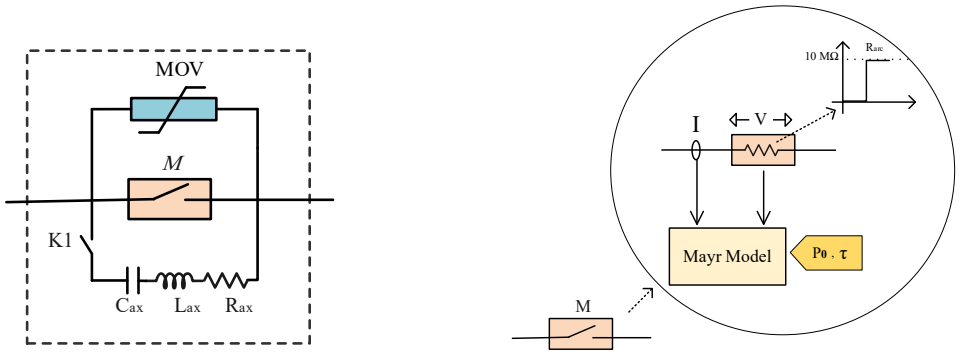


Fig. 4. Simplified arc modeling in a DC circuit breaker and its EMTDC implementation, neglecting TRV and arc restrike phenomena.

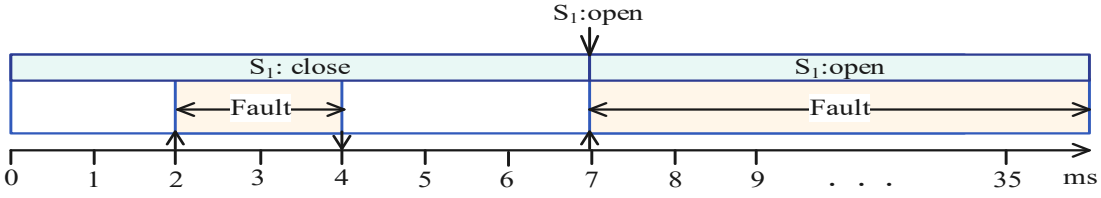


(a) Breaker arc model (b) P-MCB model

Fig. 5. Models used for the circuit breaker: (a) Breaker arc model; (b) P-MCB model

3) Modeling of FC-SFCL and Performance Simulation

To better understand the operating mechanism of the FC-SFCL under transient conditions, the analysis of magnetic flux distribution and the switching sequence of the internal switch is essential. In flux-coupled structures, the current-limiting performance strongly depends on the flux distribution within the core and the variation of magnetic coupling conditions. Therefore, a combined analysis of the time-domain behavior and magnetic flux patterns can effectively describe the transition from normal operation to the current-limiting state. Accordingly, the time sequence of FC-SFCL operation and the corresponding flux distribution in the core, illustrating the flux-locking mechanism, are presented in Fig. 6. As shown in the timing diagram of Fig. 6(a), two fault intervals are considered. In the first interval, from $t = 2$ ms to $t = 4$ ms, switch S_1 remains closed. Due to the differential winding configuration, the magnetic fluxes in the two coils largely cancel each other, resulting in a low equivalent impedance, i.e., a flux-locking state. As illustrated in Fig. 6(b), no significant net flux is established in the core, and therefore, the effective inductance L is negligible, rendering the FC-SFCL essentially inactive. In the second interval, starting from $t = 7$ ms, a fault occurs, and the switch S_1 is rapidly opened. The device transitions from a low-impedance state to a current-limiting state, increasing effective inductance and a consequent reduction in di/dt. The effect of switch opening and the variation in flux density within the core are illustrated in Fig. 6(c).



(a)



(b) (c)

Fig. 6. FC-SFCL operating sequence and core flux distribution: (a) switching/fault timing of S_1; (b) initial magnetic flux density in the core ($t < 7$ ms); (c) magnetic flux density at the end of the simulation ($t = 35$ ms).

Although flux-coupled SFCL (FC-SFCL) structures can limit the rate of rise of fault current (*di/dt*) in the initial stage of a fault through magnetic coupling mechanisms, their ability to fully suppress fault current and maintain long-term current limiting performance may be limited. In this context, incorporating a resistive superconducting element into the FC-SFCL structure can significantly enhance its performance. The resistive component, by entering the superconducting quench state, rapidly increases the effective impedance of the device. This not only further reduces the peak fault current but also prevents sustained current growth. This feature is particularly important in MVDC/HVDC systems, where fault currents exhibit extremely high rising rates. Moreover, the presence of the resistive branch improves transient damping, reduces electrical stress on protection equipment, and enhances the operating conditions of DC circuit breakers. Consequently, the combination of magnetic coupling and superconducting resistive behavior makes the FC-SFCL an effective solution for fault conditioning and improving the reliability of DC protection systems. Fig. 7 compares the dynamic behavior of the baseline and modified FC-SFCL models under DC fault conditions. Column (a) corresponds to the baseline FC-SFCL, while column (b) represents the modified structure, which includes an additional superconducting resistive element. Figures (a.1) and (b.1) illustrate the line current and FC-SFCL coil current before and after the opening of switch S_1, following the scenario described in Fig. 6. If switch S_1remains closed, no significant flux is established in the core and the FC-SFCL has negligible effect on the system. When $S_1$is opened, the baseline model mainly exhibits inductive behavior: it reduces *di/dt*, but has limited impact on the peak fault current. In contrast, the modified model achieves both reduced di/dt and a significant reduction in peak fault current due to the quenching of the superconducting element and its transition to the normal resistive state. In Figs. (a.2) and (b.2), after the opening of S_1, the flux linkage λ increases and remains relatively high in the baseline model, indicating dominant energy storage in the magnetic field (inductive behavior). However, in the modified structure, λ initially increases but subsequently decays to a lower steady-state value.

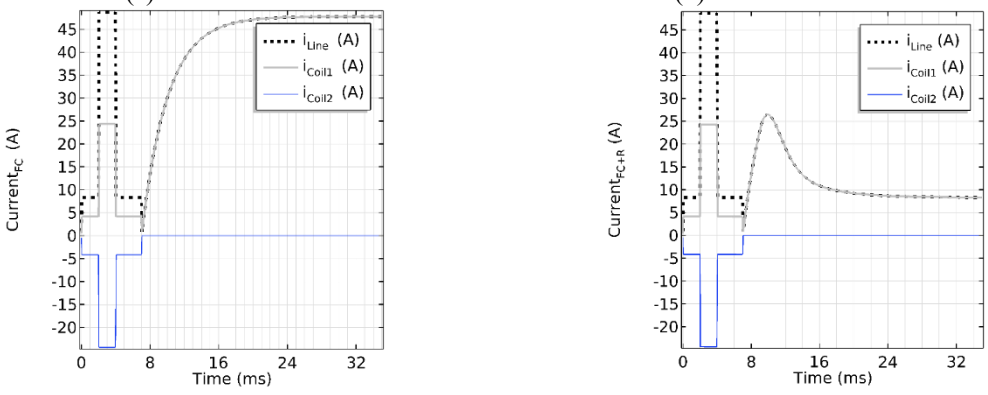
In summary, the baseline FC-SFCL primarily conditions the fault current through an inductive mechanism, increasing the effective inductance and limiting the rate of current rise, thereby providing sufficient time for the circuit breaker to operate. In contrast, the modified FC-SFCL introduces an additional resistive component that damps the transient response and provides more suitable coordination with DC circuit breakers. By also limiting the peak fault current, the modified topology becomes a more effective and practical solution for MVDC/HVDC applications.

4) Simulation of FC-SFCL Combined with Passive Mechanical DC Circuit Breaker (P-MCB)

In this section, the qualitative impact of the superconducting fault current limiter (FC-SFCL) on key performance indices of the DC circuit breaker is evaluated, including peak fault current, arc energy, transient overvoltage, and interruption time. In addition, the effect of fault location is investigated under both conditions: with and without FC-SFCL.

For this purpose, the coordinated operation of the FC-SFCL and the passive mechanical circuit breaker (P-MCB) is analyzed in a 100 kV DC system. Upon fault occurrence, the FC-SFCL modifies the system

(a) FC-SFCL (b) FC-SFCL modified



(a.1) (b.1)

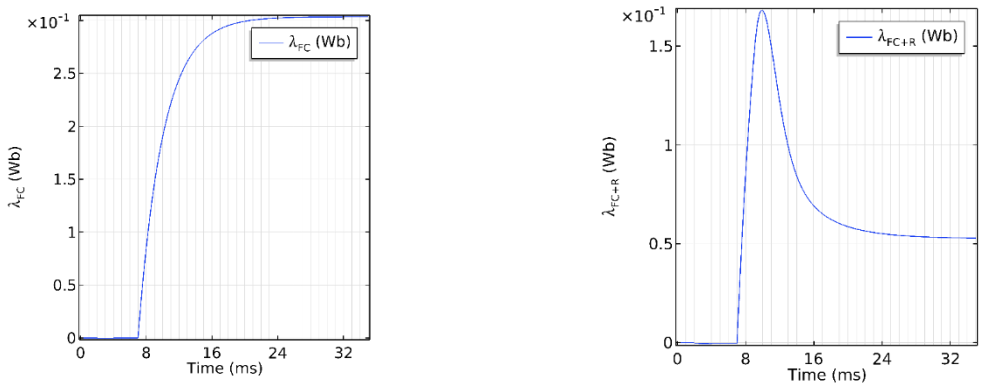


Fig. 7. Comparison of (a) baseline and (b) modified FC-SFCL models ,(a1–b1) line and coil currents; (a2–b2) flux linkage λ; (a3–b3) effective inductance L_{sc} during the fault transient.

dynamics through the switching action of S_1 and the magnetic coupling mechanism, thereby limiting both the rate of rise of fault current (di/dt) and the peak fault current. In other words, the fault condition is effectively conditioned prior to breaker operation. Subsequently, the P-MCB is

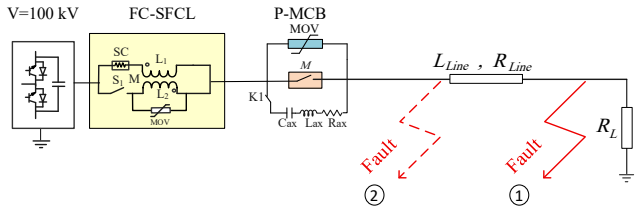


Fig.8. Test system. a) far fault (1) b) near fault (2)

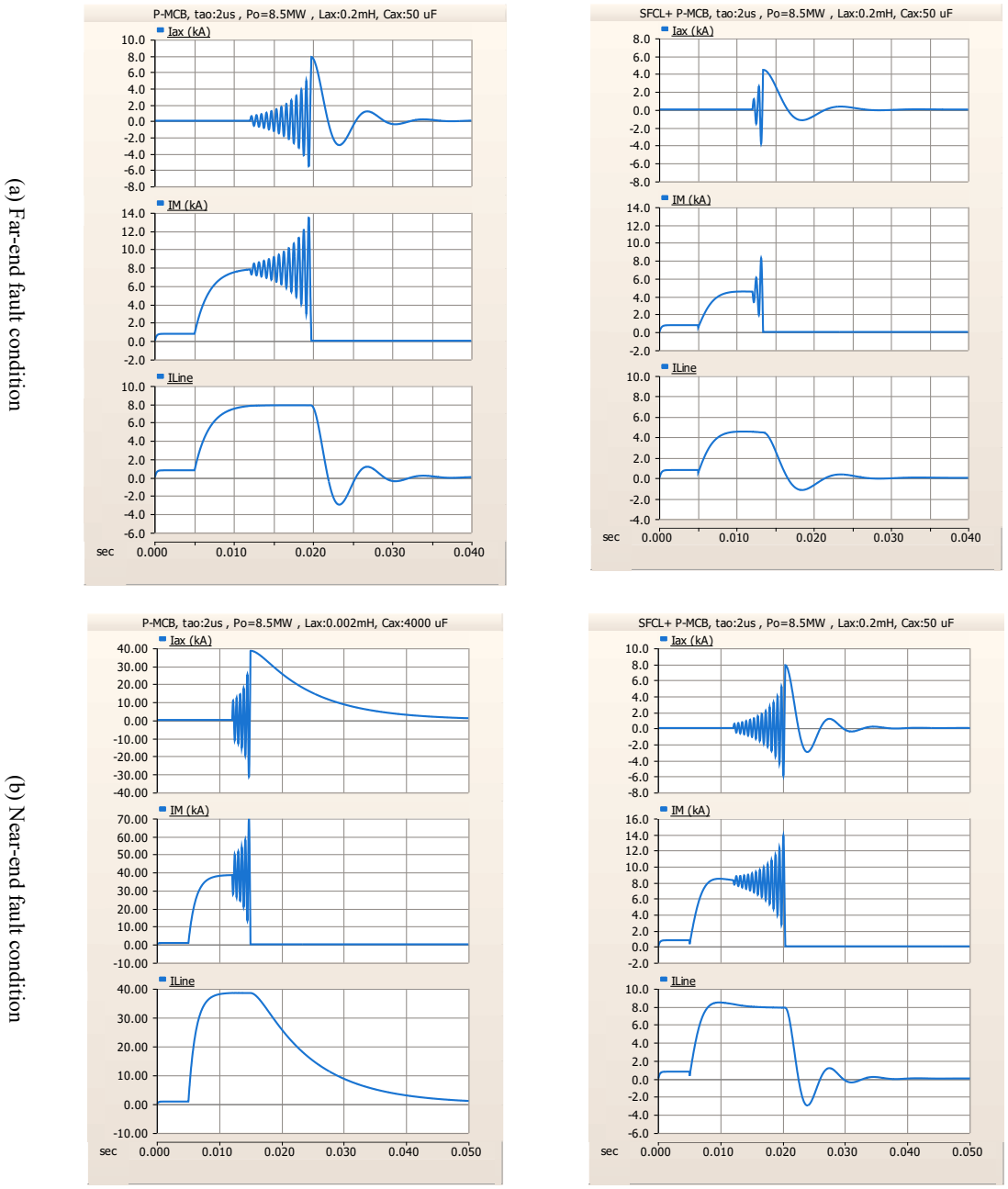
responsible for current interruption. Since the FC-SFCL reduces both the fault current magnitude and the stored energy in the system, the electrical and thermal stresses imposed on the breaker and the arc are significantly reduced. In the arc modeling, the parameters $\tau$and P_0 are kept constant for all scenarios to ensure a consistent comparison. In the P-MCB, after the opening of the main contacts M, the voltage across the breaker increases and the auxiliary branch capacitor is automatically charged. This leads to the formation of an oscillatory current in the loop consisting of the switch M and the auxiliary branch. The resulting oscillation interacts with the main current and creates a current-zero condition, enabling arc extinction and successful interruption. Fig. 8 illustrates the two fault scenarios considered in this study, namely near-end and far-end faults, which are used to evaluate the system performance. The simulation results for these scenarios are presented in Fig. 8.

Fig. 9(a) illustrates the performance of the passive mechanical circuit breaker (P-MCB) under a far-end fault condition, while Fig. 9(b) shows its operation under a near-end fault condition. In addition, both fault locations are evaluated for two cases: (i) the circuit breaker operating alone, and (ii) the circuit breaker in combination with the SFCL. The breaker parameters used in the simulation are $\tau_0 = 2\ \mu s$ and $P_0 = 8.5$ MW. The design specifications of the auxiliary branch required to achieve successful interruption are provided in Table 2.

Table 2. Comparison of L_{ax} and C_{ax} parameters under different fault scenarios.

Fault Scenario	Configuration	(L_{ax})	(C_{ax})
Far-end fault	P-MCB (without SFCL)	0.2 mH	50 µF
Far-end fault	SFCL + P-MCB	0.2 mH	50 µF
Near-end fault	P-MCB (without SFCL)	0.002 mH	4000 µF
Near-end fault	SFCL + P-MCB	0.2 mH	50 µF

In the case without the SFCL, the currents exhibit higher peaks and more severe transient oscillations, particularly at the fault inception and during the interruption process. Specifically, a large peak and significant oscillatory content are observed in I_{ax}, while $I_M$shows a pronounced overshoot, indicating increased electrodynamic stress and higher energy transfer through the interruption path. In contrast, with the inclusion of the SFCL, both the peak values and oscillation amplitudes of I_{ax}, I_M, and I_{Line} are significantly reduced, and faster transient damping is achieved.



(1) Circuit breaker only (2) Circuit breaker with SFCL

Fig. 9. Interruption performance of the circuit breaker under different fault locations and operating conditions: (1) circuit breaker only, and (2) circuit breaker with SFCL; (a) far-end fault condition and (b) near-end fault condition.

This behavior demonstrates that the SFCL increases the effective impedance during the transient period, thereby limiting di/dt and peak current magnitude, and effectively conditioning the fault before breaker operation. Consequently, the mechanical circuit breaker operates under lower current stress with a smoother transient recovery, reducing the risk of severe stress and post-interruption instability. For the near-end fault scenario without the SFCL, achieving successful interruption requires a significantly larger auxiliary capacitance. In this case, the auxiliary capacitor is increased to $C_{ax} = 4000\,\mu F$ to ensure proper current commutation and interruption capability. In practical terms, the increase in commutation capacitance reflects the requirement to provide sufficient injected current for successful interruption. The very high current levels (tens of kA in $I_M$and I_{ax}) in the case without SFCL highlight the severe challenge of interrupting near-end faults. In contrast, in the proposed hybrid FC-SFCL + P-MCB configuration, the required commutation capacitance under near-end fault conditions is reduced from $4000\,\mu F$ to $50\,\mu F$, leading to a significant reduction in electrical and thermal stress on the passive mechanical circuit breaker during the interruption process. The initial current-limiting action of the SFCL reduces the required ratings of L_{ax} and C_{ax}, enabling a more controllable interruption process with substantially smaller component values. Consequently, the peak values of I_{ax}, I_M, and the oscillatory components of I_{Line} are markedly reduced and exhibit improved damping compared with the case without SFCL. In passive resonant circuit breakers, the commutation capacitor is not independently pre-charged; therefore, expressing $I_{ax,\max}$in terms of an initial capacitor voltage V_{C0} is not strictly applicable to this topology. Instead,

I_{ax} is governed by the energy exchange between the DC system and the L_{ax} C_{ax} resonant network during commutation. The commutation dynamics are characterized by

$$\omega_0 = \frac{1}{\sqrt{L_{ax} C_{ax}}} \quad (15)$$

while the impedance ratio $Z_0 = \sqrt{L_{ax}/C_{ax}}$ determines the capability of the auxiliary branch to generate reverse current. Accordingly, under near-end fault conditions without SFCL, where I_M and di/dt are significantly high, the values of L_{ax} and C_{ax} must be appropriately tuned to enhance commutation performance. Improved commutation strength is generally achieved by reducing L_{ax} and/or increasing C_{ax}. The summary of the results corresponding to Fig. 8 is provided in Table 3.

Table 3. The summary of the results.

Parameter	Fault	P-MCB without SFCL	FC-SFCL + P-MCB	Physical Interpretation
Auxiliary branch current (I_{ax})	Far-end	Strong resonant oscillations with peak ≈ 8 kA	Reduced oscillations with peak ≈ 5 kA (≈37% reduction)	SFCL reduces the energy required for commutation, resulting in smoother and more stable current transfer.
	Near-end	Severe resonant oscillations with peak ≈ 40 kA and large reverse current	Limited to ≈ 8 kA with significantly reduced oscillations (≈80% reduction)	SFCL substantially reduces commutation energy and LC branch stress.
LC resonant behavior	Far-end	High-frequency oscillations with significant stress on auxiliary branch	Faster damping and more stable response	Initial current limitation reduces *di/dt* and transient stress in the LC network.
	Near-end	Severe high-frequency oscillations with slow damping	Well-damped and controllable oscillations	Significant reduction in transient stress due to current limiting action.
Main switch current (I_M)	Far-end	Current rises up to ≈ 14 kA with strong oscillations	Limited to ≈ 8 kA	Thermal, electrodynamic, and arc-energy stresses on the mechanical breaker are significantly reduced.
	Near-end	Current rises up to ≈ 65 kA with severe oscillations	Limited to ≈ 13 kA (≈80% reduction)	Severe reduction in breaker stress and interruption energy requirement.
Switching behavior	Far-end	High-stress and unstable interruption process	Smooth and stable current decay to zero	Arc extinction and interruption conditions are improved.
	Near-end	Highly stressed and unstable interruption	Smooth and stable interruption	SFCL improves breaker operating conditions prior to commutation.
Line current (I_{Line})	Far-end	Peak ≈ 8 kA	Reduced peak with faster damping	Increased effective impedance reduces stored energy in the system.
	Near-end	Peak ≈ 40 kA	Limited to ≈ 8 kA with fast damping	Significant reduction in system energy due to SFCL action.
Transient damping	Far-end	Slow damping with prolonged oscillations	Fast damping	Improved dynamic stability with SFCL integration.
	Near-end	Very slow damping	Fast and stable damping	Enhanced system dynamic response under severe faults.
Stress on breaker	Far-end	Moderate to high	Significantly reduced	SFCL conditions the fault prior to breaker operation.
	Near-end	Very high	Strongly reduced	Pre-conditioning of fault current improves breaker survivability.
Commutation performance	Far-end	Noticeable oscillatory commutation	Smooth and controlled commutation	Initial current limiting facilitates commutation process.
	Near-end	Severe commutation stress	Stable commutation	Improved current shaping enables controlled interruption.
Commutation network requirement	Far-end	Operates with (C_{ax}=50 μF)	Operates with (C_{ax}=50 μF)	No significant change in remote faults.
	Near-end	Requires large capacitor (C_{ax}=4000 μF)	Reduced to (C_{ax}=50 μF)	SFCL significantly reduces energy and sizing requirements of LC network.
Overall protection performance	Far-end	Moderate interruption performance	Improved reliability	FC-SFCL enhances interruption robustness.
	Near-end	Severe stress and demanding interruption	Fast, stable, and reliable interruption	Combined FC-SFCL and P-MCB significantly improves HVDC fault protection.

5) Conclusion

This paper proposes a hybrid protection scheme combining an FC-SFCL with a passive mechanical DC circuit breaker (P-MCB) for HVDC systems. The FC-SFCL effectively limits both the fault current rise rate and peak value after quenching, thereby improving the breaker operating conditions. Simulation results show that an appropriately designed FC-SFCL can reduce the peak fault current by approximately 37% under far-end faults and up to 80% under near-end faults, while significantly reducing transient

oscillations and interruption energy (I^2t). Moreover, the reduced fault current enables a substantial reduction in the required commutation capacitance, leading to a more robust interruption process with lower electrical, thermal, and electrodynamic stresses. Overall, the proposed scheme relaxes commutation circuit design constraints, reduces sensitivity to fault location, and provides a practical and reliable protection solution for future HVDC and MVDC grids.

A limitation of this study is the use of equivalent HVDC network models and fixed arc parameters to focus on the fundamental interaction between the FC-SFCL and the DC circuit breaker. Future work will consider more detailed system models and multi-terminal HVDC configurations to further validate the proposed approach.

REFERENCES

[1] A. Kamali and S. M. Barakati, "Enhancing the performance of active mechanical circuit breakers in HVDC systems using a superconducting fault current limiter," Electr. Power Syst. Res., vol. 247, p. 111727, Oct. 2025, doi: 10.1016/j.epsr.2025.111727.

[2] M. Aurangzeb, A. Xin, S. Iqbal, and M. U. Jan, "An Evaluation of Flux-Coupling Type SFCL Placement in Hybrid Grid System Based on Power Quality Risk Index," IEEE Access, vol. 8, pp. 98800–98809, 2020, doi: 10.1109/ACCESS.2020.2996583.

[3] Z. Li et al., "Application of Flux-Coupling-Type Superconducting Fault Current Limiter on Shipboard MVDC Integrated Power System," IEEE Trans. Appl. Supercond., vol. 30, no. 4, pp. 1–8, Jun. 2020, doi: 10.1109/TASC.2020.2986747.

[4] L. Chen, H. Chen, Z. Shu, G. Zhang, T. Xia, and L. Ren, "Comparison of Inductive and Resistive SFCL to Robustness Improvement of a VSC-HVDC System With Wind Plants Against DC Fault," IEEE Trans. Appl. Supercond., vol. 26, no. 7, pp. 1–8, Oct. 2016, doi: 10.1109/TASC.2016.2595622.

[5] M. Khakroei, A. M. Rajeooni, M. R. Pirbasti, and H. Heydari, "Performance Analysis of the Modified Flux-Coupling-Type SFCL in VSC-HVDC System," 2023 31st Int. Conf. Electr. Eng. ICEE 2023, pp. 19–24, 2023, doi: 10.1109/ICEE59167.2023.10334694.

[6] Y.-P. Kim and S.-C. Ko, "DC Current Limiting Characteristics of Flux-Coupled Type SFCL Using Superconducting Element Connected in Parallel in a DC System," Energies, vol. 14, no. 4, p. 1096, Feb. 2021, doi: 10.3390/en14041096.

[7] S. Ko, T. Han, and S. Lim, "DC Fault Current Limiting Characteristics of Flux-Lock Type SFCL With Parallel Connection of Two Coils Using Twice Quench," IEEE Trans. Appl. Supercond., vol. 33, no. 2, pp. 1–6, 2023, doi: 10.1109/TASC.2023.3253467.

[8] S.-H. Kim, C.-M. Park, S.-S. Choi, and S.-H. Lim, "DC Fault Current Limiting and Protective Relay Operation of Flux-Coupled Type SFCL-B,"IEEETrans.Appl.Supercond., pp. 1–6, 026,doi:10.1109/TASC.2026.3664030.

[9] M. Khakroei, A. M. Rajeooni, M. R. Pirbasti, and H. Heydari, "Multiphysics Simulation of the Modified Flux Coupling Type SFCL in VSC-HVDC Network" in 2024 32nd International Conference on Electrical Engineering (ICEE), May 2024, no. 2024, pp. 1–7, doi: 10.1109/ICEE63041.2024.10667710.

[10] L. Chen, Y. Li, S. Zheng, J. Wu, B. Su, and H. Chen, "Scheme Design and Performance Analysis of Flux-Coupling-Type SFCLs for Inhibiting Cascading Faults of AC/DC Hybrid Power Grids," *IEEE Trans. Appl. Supercond.*, vol. 36, no. 3, pp. 1–6,May 2026, doi: 10.1109/TASC.2025.3628287.

[11] B. I. Jung, H. S. Choi, Y. S. Cho, and D. C. Chung, "Analysis of the unbalanced fault in three-phase flux-coupling type SFCL using the symmetrical coordinate method," IEEE Trans. Appl. Supercond., vol. 22, no. 3, p. 5601305, 2012, doi: 10.1109/TASC.2012.2184510.

[12] J.-S. Kim, J.-C. Kim, and S.-H. Lim, "Study on Protection Coordination of a Flux-Lock-Type Superconducting Fault Current Limiter Using Switches," IEEE Trans. Appl. Supercond., vol. 26, no. 4, pp. 1–4, Jun. 2016, doi: 10.1109/TASC.2016.2549551.

[13] L. Chen, C. Deng, F. Zheng, S. Li, Y. Liu, and Y. Liao, "Fault ride-through capability enhancement of DFIG-based wind turbine with a flux-coupling-type SFCL employed at different locations," IEEE Trans. Appl. Supercond., vol. 25, no. 3, pp. 1–5, 2015, doi: 10.1109/TASC.2014.2373511.

[14] O. E. Gouda, M. I. Awaad, and Z. E. Afifi, "Impact of Superconducting Current Limiter on the Gaseous HVDC Circuit Breakers Characteristics," Electr. Power Syst. Res., vol. 199, p. 107442, Oct. 2021, doi: 10.1016/j.epsr.2021.107442.

[15] J. Xu, M. Feng, and C. Zhao, "Modular Reciprocating HVDC Circuit Breaker with Current-limiting and Bi-directional Series-parallel Branch Switching Capability," J. Mod. Power Syst. Clean Energy, vol. 8, no. 4, pp. 778–786, 2020, doi: 10.35833/MPCE.2019.000292.

[16] O. E. Gouda, D. K. Ibrahim, and A. Soliman, "Parameters affecting the arcing time of HVDC circuit breakers using black box arc model," IET Gener. Transm. Distrib., vol. 13, no. 4, pp. 461–467, Feb. 2019, doi: 10.1049/iet-gtd.2018.6264.

[17] M. Walter and C. Franck, "Improved Method for Direct Black-Box Arc Parameter Determination and Model Validation," IEEE Trans. Power Deliv., vol. 29, no. 2, pp. 580–588, Apr. 2014, doi: 10.1109/TPWRD.2013.2283278.

[18] S. Jiang, "Breaker Arc," pp. 1–12, 2018, [Online]. Available:https://hvdc.ca/uploads/knowledge_base/pscad_model_report_breaker_arc.pdf?t=1539287577.

BIOGRAPHY



Ali Kamali was born in Bandar Abbas, Iran, in 1980. He received the M.Sc. degree in Electrical Power Engineering from the University of Sistan and Baluchestan, Iran, in 2013, and is currently pursuing the Ph.D. degree in the same field at the same university. His research interests include high-voltage direct current (HVDC) circuit breakers and superconducting fault current limiters. He has experience working with advanced power system simulation and analysis tools, including MATLAB and COMSOL Multiphysics.



S. Masoud Barakati received the B.Sc. and M.Sc. degrees from Mashhad University and Tabriz University, Iran, in 1993 and 1996, respectively, and the Ph.D. degree from the University of Waterloo, Canada, in 2008. He is currently a Professor at the University of Sistan and Baluchestan, Iran. He held an Associate Research position at the University of Wisconsin–Madison, USA (2008–2009), and served as a Visiting Professor at Ryerson University and École Polytechnique de Montréal, Canada. He is currently the Editor-in-Chief of the IECO Journal. His research and industrial experience focus on microgrids, power electronics, and renewable energy systems, including the design and analysis of solar and wind power plants, distributed generation integration studies, and power electronic converter systems.